ISHELL TECHNICAL NOTE

IMAGE QUALITY ANALYSIS: @ SLIT

Original Author: Tim Bond
Latest Revision: Tim Bond
Approved by: XX

NASA Infrared Telescope Facility
Institute for Astronomy
University of Hawaii

Revision History

Revision No.	Author & Date	Approval & Date	Description
Revision X	Tim Bond Oct 8/12	Tim Bond Oct 8/12	Preliminary Release.

Contents

1 Introduction / Document Purpose

The purpose of this report is to document the details of the procedures that were undertaken to analyze the image quality of the ISHELL instrument optical design up to the slit. In particular, the effects of potential misalignments of all of the optical elements in the path up to the slit are examined.

There is a top level science requirement that the image quality of the optics up to the slit may not degrade the best seeing limited images by more than 5%.

Several factors can contribute to this image degradation. These include the telescope itself, the design residual of the optics within the instrument, the potential misalignment errors, and the fabrication errors. This analysis will quantitatively examine the effects of the misalignment of the optical elements on the image quality. Several metrics will be examined and the results presented in tabular for all of the considered metrics.

Typically the misalignments that we are modeling would originate from three different sources: the initial fabrication and alignment errors, the thermal effects from the large temperature changes, and the flexural effects from the changes in orientation.

2 Summary of Analysis Procedures

The bulk of the analysis is performed using the optical design software package – ZEMAX. Both the telescope and the instrument are modeled within ZEMAX and a complete tolerance analysis is performed. Several iterations of the analysis are undertaken, and tolerance parameters are modified appropriately in order to determine to system's sensitivity to misalignment.

In summary, the following steps were performed:

- [2.1] The original optical design in ZEMAX is modified to enable the application of tolerances to the design in such a way that realistic mechanical tolerances are in fact being modeled.

- [2.2] The tolerance analysis is run in a "sensitivity" type mode, in order to determine which elements have the most dramatic effect on the image quality when misaligned.

- [2.3] The individual tolerances are established and placed on the relevant optical elements. The tolerance analysis is then performed in a "Monte Carlo" type mode with 25 trials. Based on the results, the tolerances are fine-tuned and the Monte Carlo analysis is repeated. Several iterations of this step are performed as necessary.

- [2.4] When the final tolerances are established, a concluding "Monte Carlo" run is performed with 1000 trials. The 95th percentile of this run is examined to confirm the tolerances are appropriate. The results of the 95^{th} percentile case are examined in depth along with all the other included effects (telescope effects, optical design residual effects, and fabrication effects) and compared to the "total allowable image degradation" specification.

Note that a discussion of the appropriateness of the use of a statistical analysis is provided in Appendix A.

2.1 Refinement of the original ZEMAX design

Similar to what was done for the secondary / cold stop misalignment analysis; the original ZEMAX optical design file needed to be adapted into what was required for a full rigorous image quality analysis. Several modifications needed to be made in order to get the design into a suitable form.

2.1.1 Addition of an Entrance Pupil Location:

During normal use of the telescope it is standard procedure to "re-point" the telescope in order to maintain alignment on selected objects on the sky. By use of a coordinate break inserted at the telescope entrance pupil, we are able to simulate this procedure within ZEMAX during the tolerance runs.

2.1.2 Instrument (Optical Bench) Flexure Simulation:

As the telescope slews to different locations on the sky, the instrument moves into different orientations with respect to gravity. As this occurs, the mass of the instrument will invariably flex the main mounting trusses of the instrument, and the optical bench will move relative to the vacuum jacket and telescope. This was modeled in ZEMAX with the addition of several coordinate breaks, and by estimating the final instrument center of gravity location. It is assumed that the trusses are designed to hold the optical bench about the center of gravity.

2.1.3 Mirror Deflections:

Additional coordinate breaks were added around mirrors in order to correctly simulate the deflections of these mirrors within their mounts. Only relevant deflections were modeled (i.e. flat mirror decentration was ignored as well as axial rotations).

2.1.4 Image Rotator Flexure Simulation:

Similar to the instrument flexure, as the telescope slews to different locations on the sky, the instrument moves into different orientations with respect to gravity. As this occurs, the image rotator as a whole will flex with respect to the optical bench. This was modeled in ZEMAX with the addition of several coordinate breaks, and by estimating the final image rotator center of gravity location. Again, it is assumed that the image rotator flexes about the center of gravity.

2.1.5 Lens Barrel Flexure Simulation:

Similar to the instrument flexure, as the telescope slews to different locations on the sky, the instrument moves into different orientations with respect to gravity. As this occurs, the lens barrels as a whole will flex with respect to the optical bench. This was modeled in ZEMAX with the addition of several coordinate breaks, and by estimating the final lens barrel center of gravity location. Again, it is assumed that the image rotator flexes about the center of gravity.

2.1.6 Customized Merit Function was developed:

The default merit functions packaged within ZEMAX are all relevant to image quality, yet alone are not useful within this analysis. A custom merit function needed to be built, that could also re-point the telescope and refocus as well as evaluate the image quality. This turned out to be a fairly simple procedure.

2.2 Sensitivity Analysis

Once the new ZEMAX file was appropriately altered, a sensitivity analysis was performed in order to determine both the relative sensitivity of the image quality to the individual element perturbations, and to get first estimates for the actual magnitude of the perturbations themselves. Actual sensitivities are given in the table below (with the most sensitive elements highlighted in red).

The sensitivities given in the table below are simply the rate of change of the merit function with respect to the perturbation identified. A smaller magnitude numbers indicates the element is "less sensitive" to perturbations than an element with a larger magnitude number. A simple default ZEMAX merit function was chosen based on the resulting geometric spot sizes at the image plane.

As can be seen from the sensitivities, the tip/tilts of the individual fold mirrors, the collimator mirror, and the tip/tilt of the instrument as a whole are the most sensitive and tighter tolerances will need to be assigned to them.

Element	Sensitivity
INSTRUMENT WINDOW	
tilt about X	3.29E-06
tilt about Y	6.93E-07
INSTRUMENT FLEXURE (about CofG)	
decentration in X	2.63E-05
decentration in Y	1.18E-04
tilt about X	9.32E-04
tilt about Y	2.06E-04
rotation about Z	4.42E-05
despacing along Z	5.97E-06
FIRST FOLD MIRROR	
despacing along element axis	1.61E-05
tilt about X	1.59E-03
tilt about Y	7.04E-04
COLLIMATOR MIRROR	
despacing along element axis	4.32E-07
decentration in X	1.34E-05
decentration in Y	2.41E-04
tilt about X	3.08E-03
tilt about Y	2.22E-03
SECOND FOLD MIRROR	
despacing along element axis	1.77E-05
tilt about X	1.62E-04
tilt about Y	3.42E-04

Element	Sensitivity
IMAGE ROTATOR MECHANISM	
translation along bearing axis	1.26E-05
tilt in X of mechanism	1.76E-04
tilt in Y of mechanism	7.07E-05
decentration in X of mechanism	7.55E-11
decentration in Y of mechanism	7.52E-11
IMAGE ROTATOR F1	
despacing along element axis	1.01E-05
tilt about X	4.97E-05
tilt about Y	1.00E-04
IMAGE ROTATOR F2	
despacing along element axis	7.41E-06
tilt about X	1.65E-04
tilt about Y	4.82E-05
IMAGE ROTATOR F3	
despacing along element axis	1.01E-05
tilt about X	2.20E-04
tilt about Y	1.62E-05
THIRD FOLD MIRROR	
despacing along element axis	1.33E-05
tilt about X	4.04E-04
tilt about Y	1.73E-05

Element	Sensitivity
LENS BARREL	
translation along bearing axis	4.34E-06
tilt in X of mechanism	9.35E-05
tilt in Y of mechanism	7.70E-05
decentration in X of mechanism	6.53E-06
decentration in Y of mechanism	1.20E-04
FIRST LENS (BAF2) mounting	
despacing along element axis	6.47E-05
tilt about X	8.13E-05
tilt about Y	5.42E-05
decentration in X	1.47E-05
decentration in Y	3.70E-05
SECOND LENS (LIF) mounting	
despacing along element axis	1.45E-04
tilt about X	5.87E-06
tilt about Y	1.98E-05
decentration in X	8.17E-06
decentration in Y	1.57E-04
FOURTH FOLD MIRROR	
despacing along element axis	1.51E-05
tilt about X	1.46E-03
tilt about Y	7.02E-05

2.3 Determination of Tolerances

After several iterations on the Monte Carlo analyses (using only 25 samples), a final set of tolerances were converged upon that seemed reasonable based on semi-precision manufacturing tolerances and realistic flexure requirements (see Appendix B).

A final Monte Carlo Analysis was run with 1000 samples. The summary statistics were determined for the 95th percentile case and saved for later analysis.

The final misalignment tolerances are summarized in the chart below.

INSTRUMENT WINDOW	**IMAGE ROTATOR MECHANISM**	**LENS BARREL**
+/- 0.03 deg tilt about X	+/- 0.300 mm translation along bearing axis	+/- 0.300 mm translation along bearing axis
+/- 0.03 deg tilt about Y	+/- 0.22 deg tilt in X of mechanism	+/- 0.3 deg tilt in X of mechanism
	+/- 0.22 deg tilt in Y of mechanism	+/- 0.3 deg tilt in Y of mechanism
INSTRUMENT FLEXURE (about CofG)	+/- 0.400 mm decentration in X of mechanism	+/- 0.300 mm decentration in X of mechanism
+/- 0.600 mm decentration in X	+/- 0.400 mm decentration in Y of mechanism	+/- 0.300 mm decentration in Y of mechanism
+/- 0.600 mm decentration in Y	**IMAGE ROTATOR F1**	**FIRST LENS (BAF2) mounting**
+/- 0.22 deg tilt about X	+/- 0.150 mm despacing along element axis	+/- 0.150 mm despacing along element axis
+/- 0.22 deg tilt about Y	+/- 0.15 deg tilt about X	+/- 0.15 deg tilt about X
+/- 0.25 deg rotation about Z	+/- 0.15 deg tilt about Y	+/- 0.15 deg tilt about Y
+/- 0.600 mm despacing along Z	**IMAGE ROTATOR F2**	+/- 0.150 mm decentration in X
	+/- 0.150 mm despacing along element axis	+/- 0.150 mm decentration in Y
FIRST FOLD MIRROR	+/- 0.15 deg tilt about X	**SECOND LENS (LIF) mounting**
+/- 0.300 mm despacing along element axis	+/- 0.15 deg tilt about Y	+/- 0.150 mm despacing along element axis
+/- 0.22 deg tilt about X	**IMAGE ROTATOR F3**	+/- 0.15 deg tilt about X
+/- 0.22 deg tilt about Y	+/- 0.150 mm despacing along element axis	+/- 0.15 deg tilt about Y
	+/- 0.15 deg tilt about X	+/- 0.150 mm decentration in X
COLLIMATOR MIRROR	+/- 0.15 deg tilt about Y	+/- 0.150 mm decentration in Y
+/- 0.300 mm despacing along element axis		
+/- 0.250 mm decentration in X	**THIRD FOLD MIRROR**	**FOURTH FOLD MIRROR**
+/- 0.250 mm decentration in Y	+/- 0.250 mm despacing along element axis	+/- 0.250 mm despacing along element axis
+/- 0.22 deg tilt about X	+/- 0.25 deg tilt about X	+/- 0.25 deg tilt about X
+/- 0.22 deg tilt about Y	+/- 0.25 deg tilt about Y	+/- 0.25 deg tilt about Y
SECOND FOLD MIRROR		
+/- 0.250 mm despacing along element axis		
+/- 0.25 deg tilt about X		
+/- 0.25 deg tilt about Y		

2.4 Allowable Image Degradation

In order to determine if the tolerances were tight enough, the results of the Monte Carlo analysis needed to be compared to some image quality metric. That metric was derived from the image quality specification stated in Section 1 (that the best seeing limited image could not be degraded by more than 5%). It has long been common knowledge that the best images at the IRTF (at 2.2 µm) have a FWHM of approximately 0.4 arcsec. This observation is justified quantitatively with the calculations shown in Appendix C.

Using the basic optical parameters of the telescope and assuming a resulting Gaussian image profile, we can then specify the FWHM, 50%EE, 80%EE, and rms spot size of the image at the slit in microns. Note that the telescope focal plane is reimaged (1:1) at the slit. These values are determined in Appendix D and presented in the chart below in column two.

It is simply a case now of determining the equivalent Gaussian profile that will give a 5% image degradation when added in quadrature with the 0.4 arcsec specification. The results of that process are tabulated in columns three and four of the following chart:

Image Evaluation Criteria	*Seeing Limited Image at Slit (Assuming Gaussian)*	*Seeing Limited Image + 5% Image Degradation*	*Equivalent Gaussian to give 5% Image Degradation*
FWHM	225.88 µm	237.17 µm	74.02 µm
50% EE	225.88 µm	237.17 µm	74.02 µm
80% EE	344.14 µm	361.35 µm	110.19 µm
σ (rms spot size)	95.92 µm	100.72 µm	30.72 µm

Thus, the total allowable image degradations (including telescope effects, optical design residual, alignment, and fabrication) can be characterized as one that produces a Gaussian with a FWHM < 74.02 µm or an rms spot size of no larger than 30.72 µm.

3 Analysis Results

3.1 Results Summary

A table with the individual contributions to the total error budget is presented below:

Image Evaluation Criteria	*Telescope Contribution*	*ISHELL Optical Design*	*ISHELL Alignment Tolerances*	*ISHELL Fabrication Tolerances*	*TOTAL BUDGET*
FWHM	0.16 µm	26.8 µm	30.5 µm	TBD	**74.02 µm**
50% EE	0.16 µm	26.8 µm	30.5 µm	TBD	**74.02 µm**
80% EE	0.48 µm	33.4 µm	39.9 µm	TBD	**110.19 µm**
σ (rms spot size)	0.18 µm	13.9 µm	17.5 µm	TBD	**30.72 µm**
Strehl ratio	1.00	0.98	0.96	TBD	**0.95?**

3.1.1 Image Quality: Error Budget Contributions

The nominal telescope optical design was examined within ZEMAX and the geometric contributions determined (see Appendix E). The contributions were extremely small, but were presented regardless. The results are tabulated in column two of the table above. Note that this is a "nominal" telescope optical design and does not account for the fabrication errors, misalignment errors, or any other real world effects such as seeing. Also (**and most importantly**) the diffractive effects are ignored.

Once the ZEMAX model of the instrument up to the slit was finalized, getting the image quality specifications out of the design was trivial. The optical design residual of the telescope and the instrument up to the slit are included in the chart above, tabulated in column three. Note that the contributions are presented in a "cumulative" fashion as it would be somewhat difficult to model the instrument without the telescope.

As the tolerance analysis was being performed, it was possible to save all of the Monte Carlo cases for later examination. We then examined the 95th percentile case with all of its slightly "perturbed" elements. The image degradations from the 95th percentile case are presented in column four of the above table.

Not yet included within the above budget are the fabrication errors for the optical elements. Of these fabrication errors, the biggest portion is anticipated to be the irregularity specifications for the individual surfaces of all of the included elements. These need to be examined separately and confirmed to be small enough not to exceed the total allowable budget.

3.1.2 Image Quality: Proportions

The proportion of the individual components contribution to the total error budget is shown in the figure below.

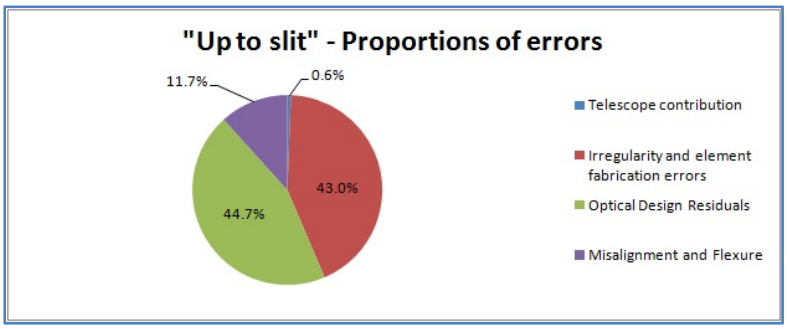

4 Appendices

4.1 Appendix A: Discussion of the Statistical Analysis

4.1.1 Distribution Form of Individual Tolerances:

During the Monte Carlo analysis, the value for each of the individual perturbations is chosen from a probability density. ZEMAX allows the user to select from several predefined distributions (Gaussian, Uniform, and Parabolic) or to even specify a custom distribution. The default is Gaussian, but we chose to switch to a parabolic distribution as this would more accurately model real world manufacturing processes.

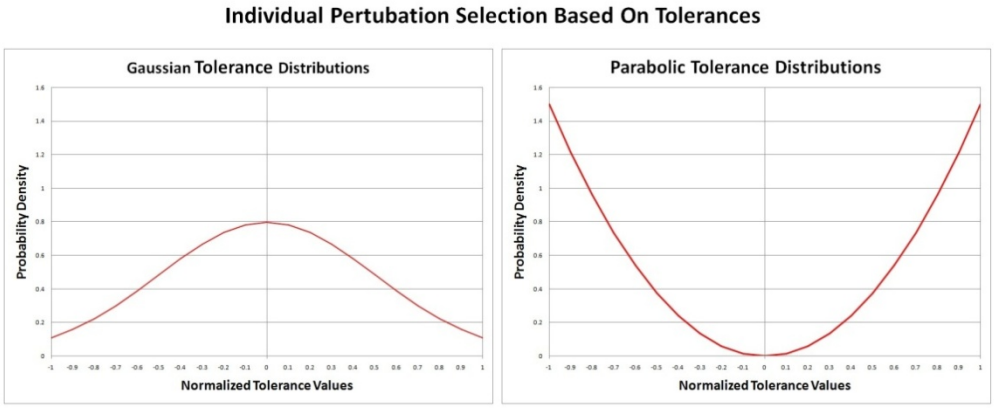

4.1.2 Use of the 95th Percentile Standard:

Due to the large number of tolerances involved and the random nature in which they are likely to interact with each other, a statistical analysis of these tolerances is utilized. If all of the tolerances were simply "stacked" as would be done in a worst case scenario, it would simply be too difficult (and expensive) to meet the desired requirements. It is standard practice in the optics industry to employ a statistical tolerance scheme to help relax some of the tolerances that need to be attained.

In our case, the mean result is reported (expected value) as well as the 95th percentile case (within 2 standard deviations).

4.2 Appendix B: Example Tolerance Considerations

The following general calculations are used as a basis for determining reasonable tolerances.

CASE 1: A 15um deflection over 40mm baseline

A typical optical element diameter is 40mm and it may be possible to hold the deflections on one edge of that element to a potential 15um.

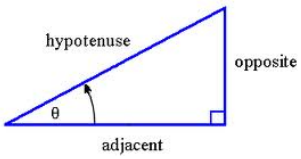

$$\emptyset = \tan^{-1}\left(\frac{opposite}{adjacent}\right)$$
$$\emptyset = \tan^{-1}\left(\frac{0.015}{40.0}\right)$$
$$\emptyset = 0.021°$$

CASE 2: A 250um deflection over 750mm baseline

The distance from the center of gravity of the instrument out to one of its extreme ends is 750mm and it may be possible to hold the deflections on one edge of the instrument to a potential 250um.

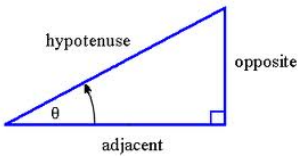

$$\emptyset = \tan^{-1}\left(\frac{opposite}{adjacent}\right)$$
$$\emptyset = \tan^{-1}\left(\frac{0.250}{750.0}\right)$$
$$\emptyset = 0.019°$$

CASE 3: Total Instrument deflections might be in the range of ±0.150mm

Considering, for example a total instrument mass of 500kg and a G10 support truss system with 2 arms. It is conceivable that each arm might carry loads up to:

$$F = \frac{1}{2}(500)(9.81) \quad \Leftrightarrow \quad F = 2452\ N$$

Considering members that are 50mm x 12.5mm x 500mm long, with a Young's Modulus of E=18.0 GPa, one can expect deflections of the order:

$$\delta = \frac{(2452)(0.500)}{(0.050)(0.0125)(18.0 \times 10^6)} \quad \Leftrightarrow \quad \delta = 0.109\ mm$$

Note: this only accounts for the elongation/compression of the truss member. Lateral flexure is usually significantly higher than the elongation/compression component.

4.3 Appendix C: Mauna Kea Seeing Calculations:

As per Mark Chun – MK Survey results, the following seeing conditions can be expected for the Mauna Kea summit. All are given at 0.5 µm and are based solely on atmospheric seeing.

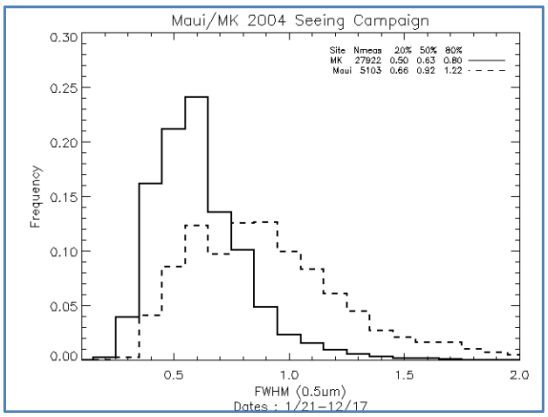

20th percentile = 0.5 arcsec

50th percentile = 0.63 arcsec

80th percentile = 0.8 arcsec

Relevant Equations for converting to 2.2 µm:

$$FWHM = \frac{0.98\lambda}{r_0} \quad \text{(radians)}$$

$$FWHM = \left(\frac{0.98\lambda}{r_0}\right) \cdot \left(\frac{3600 \cdot 360}{2\pi}\right) \quad \text{(arcsec)}$$

$$\left[\frac{(r_0 \,@\, \lambda_1)}{(r_0 \,@\, \lambda_2)}\right] = \left(\frac{\lambda_1}{\lambda_2}\right)^{\frac{6}{5}}$$

SEEING DATA FROM MARK CHUN (MK SURVEY)						
	FWHM @0.5 um (arcsec)		Ro @0.5 um (m)		Ro @2.2 um (m)	FWHM @2.2 um (arcsec)
20th %ile	0.5		0.20213951		1.196174	0.371774
50th %ile	0.63		0.160428183		0.949345	0.468436
80th %ile	0.8		0.126337194		0.747609	0.594839

Final Conclusion: Expected best seeing (20th percentile) @ 2.2 µm is ≈ 0.40 arcsec

4.4 Appendix D: Nominal Telescope Parameters:

The basic geometry of the IRTF telescope is shown in the following figure:

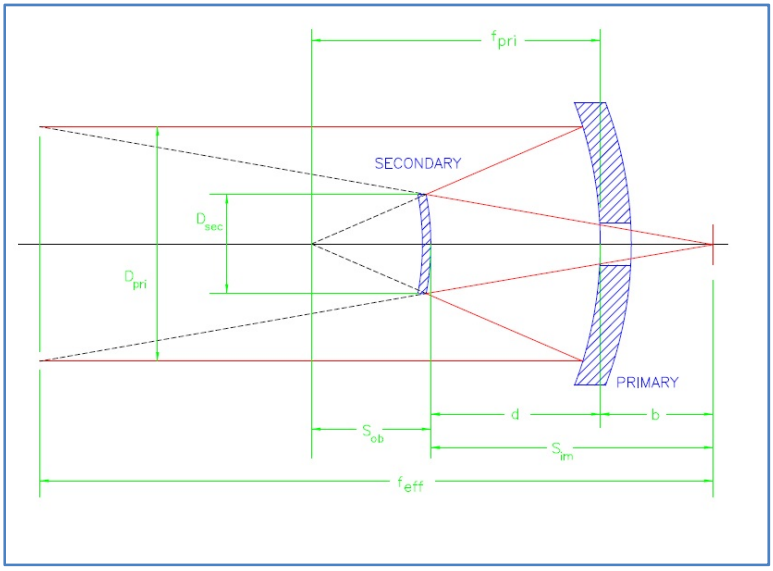

There are a variety of first order calculations that can be performed to give an indicator of the basic optical performance of the system:

PRIMARY MIRROR:
Radius of Curvature: 15 271.75
Conic Constant: -.99388
Outer Diameter: 3 218.18 mm
Inner Diameter: 1 107.44 mm

SECONDARY MIRROR:
Radius of Curvature: -1 311.529
Conic Constant: -1.206847
Outer Diameter: 244 mm
Inner Diameter: 50.8 mm

Dist (vertex primary to vertex secondary): 7 023.1 mm
Dist (vertex primary to focus): 2324.208 mm

Note that the secondary mirror is the system stop and defines the diameter of the beam footprint through the system (i.e. the primary mirror has an oversized O.D. and an undersized I.D. to accommodate different beam patches)

From the above radii of curvature, one can easily calculate the focal lengths of the primary and secondary mirrors:

$$f = \frac{1}{2}(Radius\ of\ Curvature)$$

$$f_{pri} = \frac{1}{2}(15\ 271.75) = 7\ 635.875\ mm$$

$$f_{sec} = \frac{1}{2}(1\ 311.529) = 655.7645\ mm$$

It can be shown that for a two lens (mirror) system the effective focal length is given by the following equation:

$$f_{eff} = \frac{(f_{pri})(f_{sec})}{[f_{pri} + f_{sec} - d]}$$

$$f_{eff} = \frac{(7635.875)(655.7645)}{[7635.875 + 655.7645 - 7023.1]}$$

$$f_{eff} = 116\,476.86 \text{ mm}$$

The image scale at the focal plane can then be determined as follows:

$$Image\ Scale = \frac{f_{eff}}{206\,264.8}$$

$$Image\ Scale = 0.5647\ mm/arcsec$$

And thus a 0.4 arcsec seeing limited image at the telescope focal plane would have:

$$FWHM = (0.5647)(0.4)$$
$$FWHM = 225.88\ \mu m$$

If a Gaussian profile is assumed for the image, the following parameters can also be stated:

$$50\%EE = FWHM = 225.88\ \mu m$$

$$80\%EE = \frac{1.621}{1.064} FWHM = 344.14\ \mu m$$

$$rms\ spot\ size\ (\sigma) = \frac{0.4517}{1.064} FWHM = 95.92\ \mu m$$

4.5 Appendix E: IRTF "Telescope Only" Image Quality:

Using the "nominal parameters" for the IRTF telescope optical prescription, a ZEMAX model was constructed and the "nominal" image quality was determined. In ZEMAX, there is no provision for adding atmospheric turbulence and so these image quality derivations are "theoretical" in a sense that they are what can be achieved in the absence of any atmospheric image degradation.

Two sets of results are given. First, the geometric analysis is presented. This analysis is somewhat simplified and considers only the individual rays as they pass through the system. **It does not consider diffraction effects.** These are the results that are used in determining the image quality throughout the instrument.

Next an analysis is performed that also considers diffractive effects. This is done for reference only and results are given to give the reader a sense of "what may be possible" if the effects of the atmosphere were completely removed.

4.5.1 Geometric Analysis

Using the ZEMAX model of the telescope, the following spot diagram and encircled energy diagrams were found:

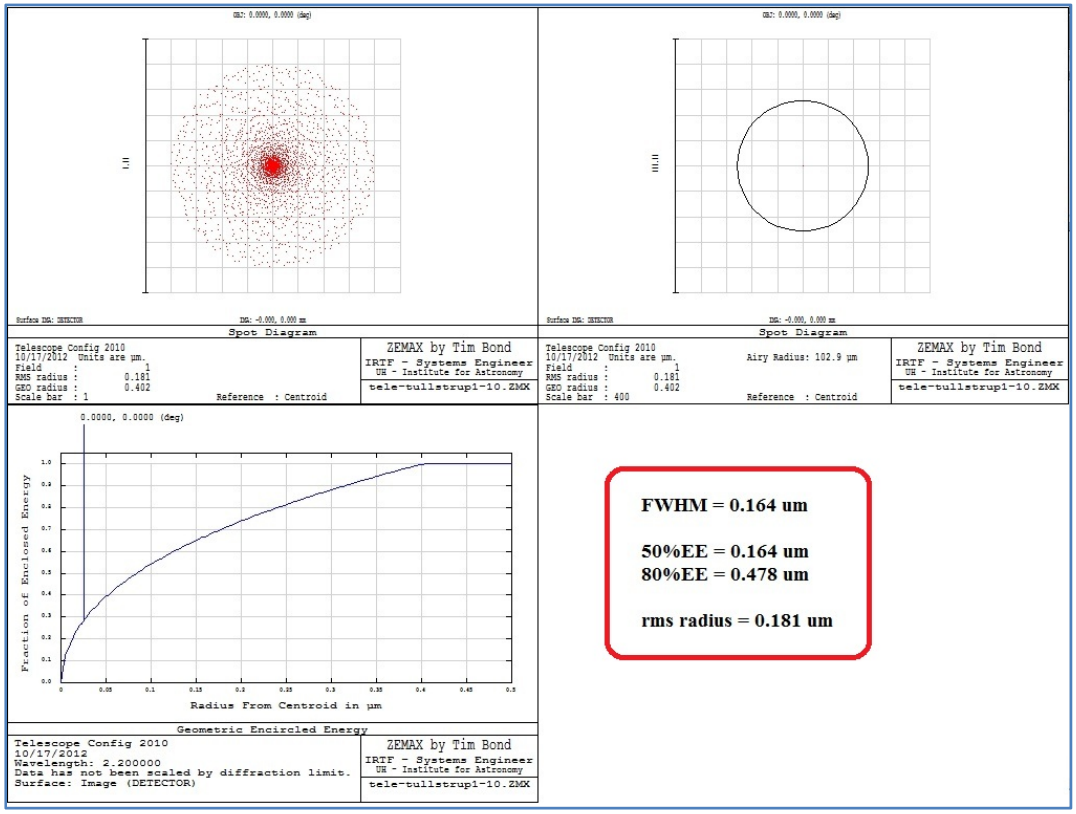

Note again, that the above image quality is for the telescope alone and does not consider diffraction effect.

4.5.2 Physical Wave Optics Analysis

Using the ZEMAX model of the telescope is analyzed considering diffractive effects, the following point spread function (PSF), wavefront error, and encircled energy plots are found:

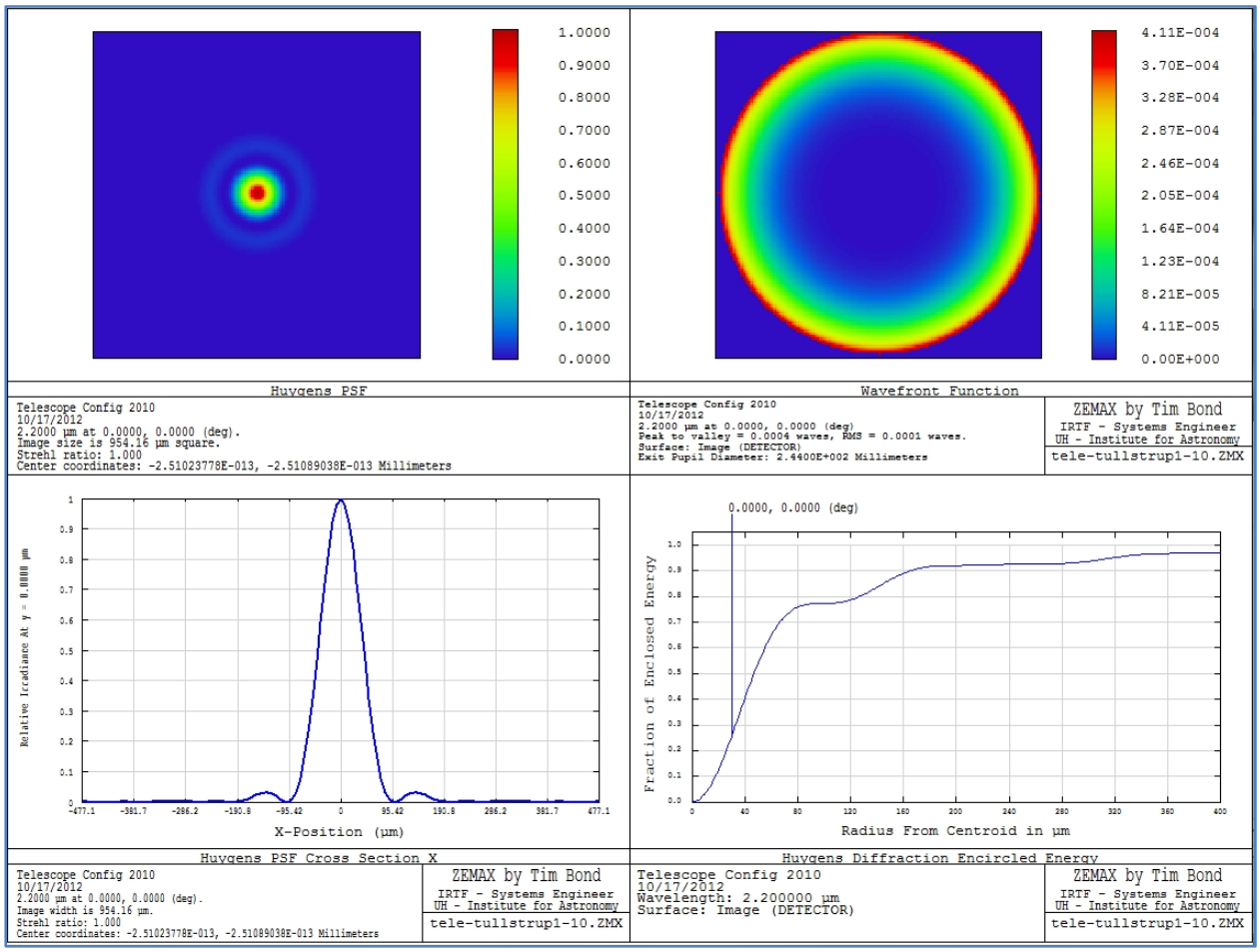

And the following parameters are resultant

FWHM = 85.0 µm
50%EE = 93.2 µm
80%EE = 252.4 µm
rms spot size (σ) = 37.32 µm (Best "Gaussian" match)
Strehl ratio = 1.00

Note that this is in excellent agreement with what one would expect for the Airy FWHM = 86.7 um (at 2.2 um)